ACS OMEGA

Article

Cite This: ACS Omega 2018, 3, 10139−10144

http://pubs.acs.org/journal/acsodf

One-Step Fabrication of Bioinspired Lubricant-Regenerable Icephobic Slippery Liquid-Infused Porous Surfaces

Yizhi Zhuo, Feng Wang, Senbo Xiao, Jianying He,* and Zhiliang Zhang*

NTNU Nanomechanical Lab, Department of Structural Engineering, Norwegian University of Science and Technology (NTNU), Trondheim 7491, Norway

Supporting Information

ABSTRACT: Icephobic coating and surfaces are essential for protecting infrastructures such as transmission lines, transportation vehicles, and many others from severe damages of excessive icing. The slippery liquid-infused porous surfaces (SLIPS) are attracting escalating attention because of their low-ice adhesion strength. Despite all of the encouraging laboratory scale results, the SLIPS are still far from being applicable in real environments owing to the key unsolved problem, namely anti-icing durability. Inspired by the functionality of the amphibians' skin, lubricant regenerability was introduced to conventional SLIPS and realized by a facile and scalable fabrication route. A series of polydimethylsiloxane (PDMS)-based skinlike SLIPS were designed and fabricated by using a one-step method, the solvent evaporation-induced phase separation technique. The obtained skinlike SLIPS were able to regenerate surface lubricant constantly by internal residual stress because of phase separation and survive more than 15 cycles of wiping/regenerating tests. Thanks to the regenerability of the surface lubricant, the new SLIPS demonstrated durable icephobicity, showing a long-term low-ice adhesion strength below 70 kPa, which was only 43% of 160 kPa that for the pristine PDMS (Sylgard 184), even after 15 icing/deicing cycles. This work paves a new and facile way for achieving icephobic durability of SLIPS.

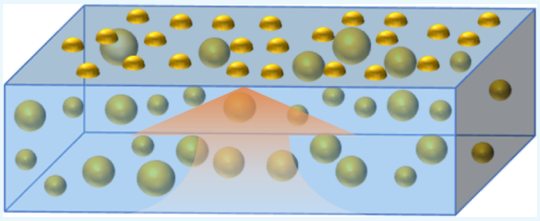

INTRODUCTION

Ice accretion on surfaces of infrastructures, transportation vehicles, and many others can result in severe damages; large-scale extreme examples of that are the 2008 Chinese winter storms and the Northeastern United States blizzard of 1978. The traditional anti-icing methods, including active heating and usage of antifreeze liquid or salt, are either too costly or environmentally harmful.[1−3] It is commonly conceived that the new generation of passive anti-icing surfaces and coatings holds a promise.[2,4] The superhydrophobic surfaces (SHS), surfaces with low surface energy, as well as micro- and/or nano-topography, have been widely investigated because of their icephobic potential of repelling coming water droplets, delaying ice nucleation, and reducing ice adhesion strength.[4−12] However, this type of surfaces were proven to lose their icephobicity in high humidity atmosphere. The SHS cannot avoid moisture condensation in their surface micro- and/or nanotexture, which leads to the wetting transition from Cassie−Baxter state to Wenzel state and finally a catastrophic increase in ice adhesion strength.[13−17] The slippery liquid-infused porous surfaces (SLIPS) have attracted increasing attention for the low-ice adhesion strength they can achieve.[18−22] The SLIPS rely on the high mobility of surface lubricant for super icephobicity and thus are free of the problems suffered in the SHS. However, the SLIPS may lose their icephobicity because of the lubricant removal by ice, in extreme case, after only one icing/deicing cycle.[23]

One of the key unsolved issues of SLIPS is to enable the surfaces to survive icing/deicing cycles, that is, anti-icing durability.[15,24−28] Most of the previous studies on SLIPS focused on their low adhesion to ice, yet only limited work had devoted to improve their durability. Recently, Liu et al. attempted to increase the durability of SLIPS via chemical modification and nanoengineering. They investigated the effects of the surface chemistry, length scale, and hierarchy of the surface topography of the underlying substrates on their ability to retain the lubricant during repetitive icing/deicing.[26] The results showed that the heptadecafluorodecyl trimethoxysilane-fluorinated hierarchically microstructured SLIPS are more durable than the ones without nanostructure and/or fluorination. Unfortunately, the ice adhesion strength of their SLIPS increased from ∼60 to 700 kPa after 20 icing/deicing cycles, which is excessively high for practical applications. Taking another approach, Coady et al. incorporated UV-cured polymer networks into SLIPS to prevent the removal of surface lubricating oil and maintain ice adhesion strength below 100 kPa for 13 deicing cycles.[23] These studies indicate the feasibility of enhanced durability of SLIPS by increasing capillary force and/or suppressing the release rate of lubricant. Despite the unremitting efforts, new approaches toward durable SLIPS are still desperately in need.

Living organisms can secrete surface lubricant and liquids, which inspires the design and fabrication of durable SLIPS. One interesting creature, the amphibians, can actively secrete

Received: May 26, 2018
Accepted: August 8, 2018
Published: August 30, 2018

DOI: 10.1021/acsomega.8b01148
ACS Omega 2018, 3, 10139−10144

mucus to maintain hydrated body surface.[29] The functionality of surface hydration refilling of amphibians is ascribed to the mucus glands that constantly wet the surface soft epidermis. It is desired to fabricate novel SLIPS with relatively simple structures, surely not as complex as skins of real animals but possess similar or same surface lubricant regenerating ability.

Immiscible liquid and a soft substrate with porous structures, which can act as mucus and soft epidermis, respectively, are essential for imitating the function of amphibian skins. Polydimethylsiloxane (PDMS) is a competent candidate for fabricating porous soft substrate because it is viscoelastic and moldable. There are a wide variety of methods for preparing porous PDMS, including direct templating,[30−32] emulsion templating,[33] gas foaming,[34] phase separation,[35,36] 3D printing technique,[37] and so on.[38] Typically, fabrication of SLIPS requires a separate step of infusing liquid into the porous substrate. Here, in this study, a simplified approach via solvent evaporation-induced phase separation for SLIPS was developed, as the details are schematically shown in Figure 1. A

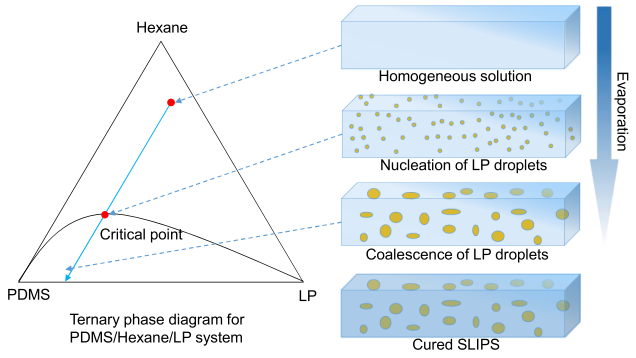

Figure 1. Schematic preparing principle of skinlike SLIPS.

homogenous solution made up of Sylgard 184, liquid paraffin (LP), and hexane is first prepared. Sylgard 184 is one kind of commercial silicone rubber, which is hydrophobic and serves as the soft substrate and continuous phase of the resulting coating. LP is the nonsolvent of PDMS and can act as the lubricant of SLIPS. The hexane is the cosolvent of PDMS and LP, which can dissolve PDMS and LP to form a homogeneous solution. Thanks to the volatility of hexane, which can evaporate at room temperature. The evaporation of hexane induces nucleation, growth, and coalescence of LP droplets, resulting in phase separation and a mixture of two phases: a continuous phase of Sylgard 184 and a dispersed phase of LP. New skinlike SLIPS were obtained after the curing process. The structure of the new skinlike SLIPS was carefully studied for elucidating the mechanism of surface lubricant regenerability. The icephobicity of the new surface was also investigated in this study. Strikingly, the new SLIPS were able to regenerate surface lubricant, LP droplets, even after 15 wiping/regenerating tests, which led to long-term low-ice adhesion <70 kPa after 15 icing/deicing cycles, outperforming many other SLIPS.

RESULTS AND DISCUSSION

Morphology of the Novel Skinlike SLIPS. The as-prepared skinlike SLIPS demonstrated a fine porous surface, as shown in Figure 2. The pores on the surface were filled with lubricant, LP droplets, which were constrained by the PDMS matrix. The size of droplets increased with increasing LP content as expected. To further investigate the influence of LP content on the pore size of the PDMS matrix, the skinlike SLIPS were first immersed in fresh hexane to soak out the LP droplets and then characterize the microstructure by scanning electron microscopy (SEM). As shown by SEM images with different scales in Figure 3, the pore sizes on the surface of the PDMS matrix of three samples (Figure 3a,b,d,e,g,h) indeed increased with the LP content, in agreement with the previous report.[35] The pore sizes in the cross section (Figure 3c,f,i) of the samples showed the similar pore size and same trend, which indicated that the pores evenly distributed in whole PDMS matrix. The pore size was measured from the SEM images, as the corresponding size distribution histograms shown in Figure 4. The distributions of pore sizes in LP-0.25 and LP-0.50 were found to be close to unimodal Gaussian distribution. In contrast, the pore size in LP-0.75 featured a bimodal Gaussian distribution, which can be ascribed to the coalescence of large LP droplets. The mean pore size increased from 0.80 to 3.78 μm with the increasing LP content (Figure 4d). High-concentrated LP is in favor of the growth and coalescence of LP droplets, which is the reason of the increasing pore size. The result indicates that the pore size of the PDMS matrix can be tuned by simply controlling the amount of LP. It should be noted that the pore size and distribution can be further regulated by controlling the curing temperature and addition of the surfactant.[35]

Regenerability of Lubricant Droplets of Skinlike SLIPS. The most interesting property of the new skinlike SLIPS is the regenerability of lubricant droplets. After the LP droplets on the surface was removed, new droplets can regenerate, grow, and coalesce on the surface. To study the regenerability of the as-prepared surfaces, an optical microscope with an integrated camera was used to record the evolution of surface morphologies after wiping off the LP droplets. As shown in Figure 5, the LP-0.25 was taken as a representative of all three samples in the lubricant-wiping experiments. Right after wiping the surface (Figure 5a), there were only some tiny droplets remaining on the surface. After 10 min growth, the size of droplets became larger with time (Figure 5b). From 10 to 30 min, the droplets kept growing and became much larger and uniform (Figure 5c). More details for this regeneration process from 0 to 30 min are shown in Video

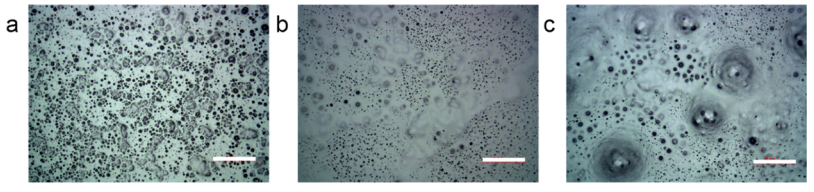

Figure 2. Optical micrographs of skinlike SLIPS: (a) LP-0.25, (b) LP-0.50, and (c) LP-0.75. Scale bar: 200 μm. The white region corresponds to the continuous phase of PDMS, whereas the darker region corresponds to the dispersed phase of LP.

DOI: 10.1021/acsomega.8b01148
ACS Omega 2018, 3, 10139−10144

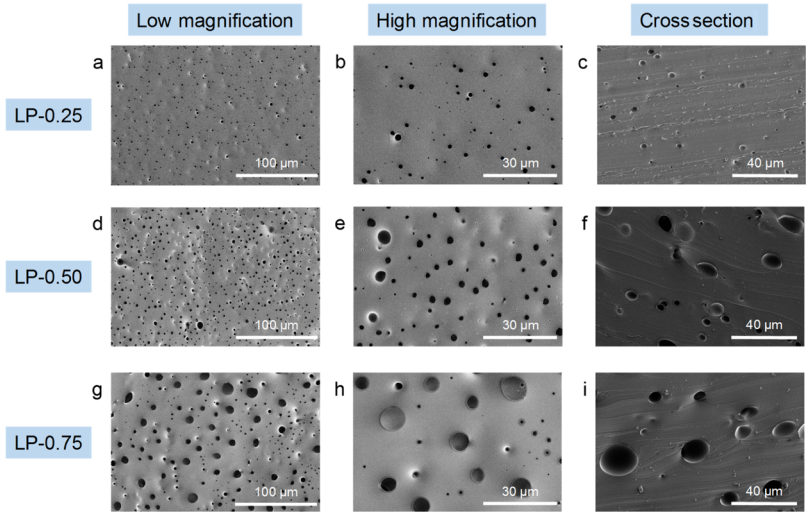

Figure 3. SEM images of the PDMS matrix. Surface morphologies in low magnification, high magnification, and the cross section of (a–c) LP-0.25, (d–f) LP-0.50, and (g–i) LP-0.75.

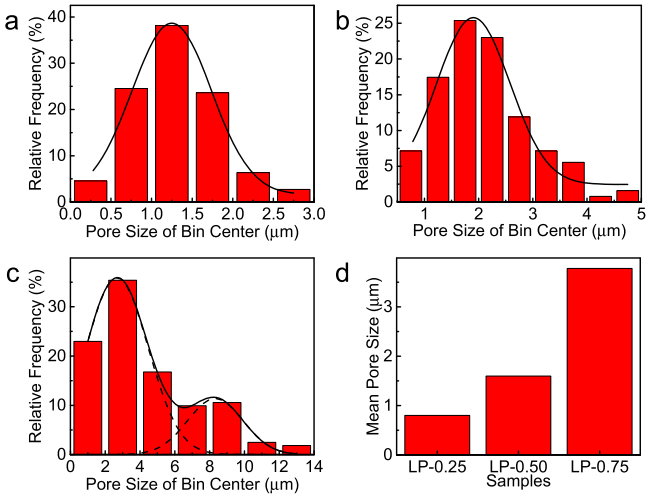

Figure 4. Pore-size distribution histograms of (a) LP-0.25, (b) LP-0.50, and (c) LP-0.75. (d) Mean pore size of samples.

S1 of the Supporting Information, which contain more frames of the evolution and demonstrated the growth of droplets. The LP inside the PDMS matrix was squeezed out leading to the growth of the droplets. When two or more adjacent droplets grew to a certain size and contact with each other, they coalesce to form a single large droplet. These coalescence events can be found in Video S2 of the Supporting Information, indicating that coalescence also contributed to the growth of droplets.

To further evaluate the durability of the skinlike surface, repeated wiping/regenerating test were conducted with all three samples. As shown in Figure 6, actively emerging LP droplets were still found on the surfaces after 15 wiping/regenerating tests, which indicates notable regenerability of the skinlike SLIPS and the success of the biomimetics in this study. Furthermore, the droplets size of LP-0.25 after 15 wiping/regenerating tests is larger than that of LP-0.50 and LP-0.75. One of the reasons for this is that more LP have been removed for LP-0.50 and LP-0.75 during wiping tests. Another reason is that the matrix of LP-0.25 can provide larger inner pressure to squeeze LP to the surface because of smaller pore size.

The mechanism of surface lubricant regenerability can be explained based on Young–Laplace equation, as illustrated in Figure 7. The driving force of the regenerability was the inner pressure (p_i) of the PDMS matrix, which resulted from the residual stress of fabricating process and larger than the atmosphere pressure (p_a).[39] The LP inside the PDMS matrix was squeezed out by the inner pressure to form droplets on the surface. With the growth and coalescence of droplets, the system reached equilibrium state because of the Laplace pressure. After wiping the LP droplets from the surface, the equilibrium state was broken; then the LP will be squeezed out again until the equilibrium state is reestablished. Hence, the regenerability can survive more than 15 wiping/regenerating test cycles.

Anti-icing Properties. Anti-icing properties of the skinlike SLIPS were investigated by characterizing the ice adhesion strength on the surfaces. There are many different methods to measure the ice adhesion strength, including horizontal shear, tensile strength, centrifugal shear, vertical shear, and so on.[25,27,40−43] Here, the ice adhesion strength on the skinlike SLIPS were tested by vertical shear test similar to our previous

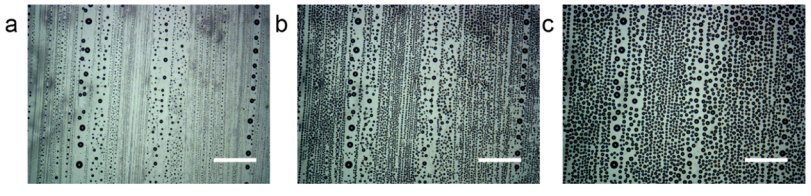

Figure 5. Optical micrographs of LP-0.25 at (a) 0, (b) 10, and (c) 30 min after wiping the LP droplets off. The droplets grow larger and larger with the time. Scale bar: 200 μm.

DOI: 10.1021/acsomega.8b01148
ACS Omega 2018, 3, 10139−10144

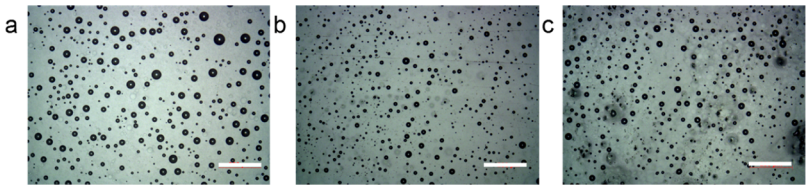

Figure 6. Optical micrographs of (a) LP-0.25, (b) LP-0.50, and (c) LP-0.75 after 15 wiping/regenerating tests. Many LP droplets are found on the surfaces after 15 wiping/regenerating tests. Scale bar: 200 μm.

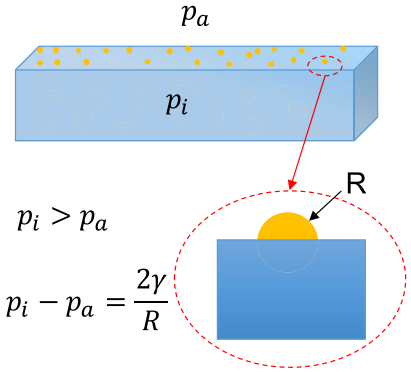

Figure 7. Schematic equilibrium state of the skinlike SLIPS. Laplace pressure makes the system in a metastable state, where p_i, p_a, γ, and R are the inner pressure of the matrix, the atmosphere pressure, surface tension of liquid, and curvature of the droplets, respectively.

reports.[40−43] As shown in Figure 8, the ice adhesion of skinlike SLIPS, LP-0.25, LP-0.50, and LP-0.75 were measured to be

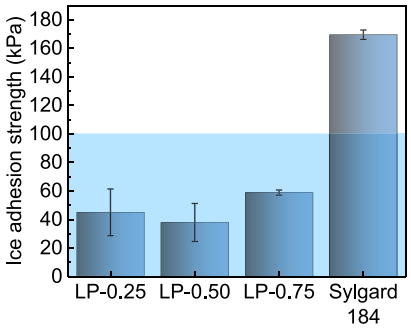

Figure 8. Ice adhesion strength of LP-0.25, LP-0.50, LP-0.75, and Sylgard 184.

45.0 ± 16.4, 37.9 ± 13.3, and 58.9 ± 1.8 kPa, respectively. As the definition of icephobic surfaces was suggested to have ice adhesion strength below 100 kPa,[15,44] all of the three samples were below the threshold and were icephobic. It should be noted that the ice adhesion strength on the skinlike SLIPS was much lower than the value of Sylgard 184 with similar thickness (300−400 μm). There are three factors which can influence the ice adhesion strength: surface elasticity, surface topography, and liquid extent.[45] For skinlike SLIPS, the low-ice adhesion strength can be attributed to modulus mismatch between ice and PDMS matrix, and more importantly, the presence of LP droplets, which can serve as lubricant and at the same time reduce the real-ice contact area. In addition, mechanical interlocking may result from the surface topography. For example, on comparing the other two surfaces, LP-0.75 shows rougher surface, which can induce mechanical interlocking; thereby, it displays higher ice adhesion strength.

Because of the high mobility of surface lubricant, previous SLIPS were not durable for anti-icing.[26] To verify the durability of the skinlike SLIPS, repeating icing/deicing experiments were carried out, as shown in Figure 9a. All of the samples were found to maintain low-ice adhesion strength below 70 kPa during 15 icing/deicing cycles, outperforming many other SLIPS.[23,26] The durability was expected, given the regenerable LP droplets on the surface as well as the slow release rate of LP because of high affinity between LP and PDMS.[46] Moreover, we collected all of the ice adhesion strength among the icing/deicing cycles and obtained the average value, as shown in Figure 9b. The average value increased with the increasing LP content, which is in agreement with the phenomenon in Figure 6 (the droplets size of LP-0.25 after 15 wiping/regenerating tests is larger than that of LP-0.50 and LP-0.75). Besides, mechanical interlocking effect is more significant in LP-0.75. In summary, the results showed that the design of skinlike SLIPS with regenerable lubricant indeed can improve the durability of SLIPS.

CONCLUSIONS

A series of new skinlike SLIPS inspired by amphibians were fabricated to solve the durability challenge by enabling the surface lubricant regenerability. The lubricant regenerability of the new surface survived more than 15 wiping/regenerating tests and resulted in a long-term low-ice adhesion strength below 70 kPa, which is only 43% of 160 kPa that for the pristine PDMS (Sylgard 184), after 15 icing/deicing cycles.

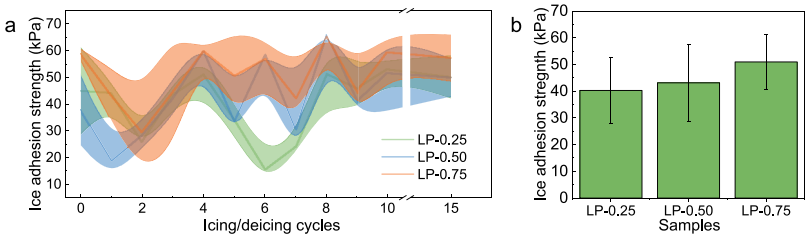

Figure 9. (a) Ice adhesion strength of skinlike SLIPS during 15 icing/deicing cycles. (b) Average ice adhesion strength of skinlike SLIPS among the icing/deicing cycles.

DOI: 10.1021/acsomega.8b01148
ACS Omega 2018, 3, 10139−10144

The low-ice adhesion strength resulted from not only the presence of lubricant but also the modulus mismatch between ice and PDMS matrix. The new SLIPS had simple composition, namely two key components of LP and PDMS as lubricant and porous substrate, respectively, fabricated by the one-step method based on the solvent evaporation-induced phase separation technique. The fabrication process provided good control on surface morphology and most importantly pore size for lubricant regenerability, as well as upscaling potential. In addition, we believe that better regeneration ability can be obtained by tuning the solvent, lubricant, curing temperature, and so on. This work paves a facile and scalable way for solving the icephobic durability issue toward practical applications of SLIPS.

EXPERIMENTAL SECTION

Fabrication of Skinlike SLIPS. The fabrication procedure is described as follows. The homogeneous solution containing 2.5 g of Sylgard 184 base, 0.25 g of LP, and 12.5 mL of hexane was first prepared in a container, with 0.25 g of Sylgard 184 curing agent charged into the mixture and stirred for 5 min. Afterward, 4 mL of the solution was cast into a homemade mold, as depicted in our previous report.[40] The solution was kept at room temperature for 60 min to allow the evaporation of hexane, followed by curing at 100 °C for another 60 min. The as-prepared surface was termed LP-*x*, where *x* is the weight (g) of LP. Herein, three SLIPSs, LP-0.25, LP-0.50, and LP-0.75 with the thickness of 300−400 μm were prepared.

Characterization. Surface morphologies of skinlike SLIPS and the evolution of surface morphologies after wiping LP droplets off were recorded by a differential interference contrast microscope with an integrated camera (Carl Zeiss, Zeiss Axioscope A1 for reflected light). SEM was conducted in the field-emission SEM (FEI Apreo SEM) to study the microstructure of porous PDMS substrates, which were sputter-coated with a 10 nm platinum layer in advance. All samples were immersed in hexane, which was refreshed every day, for 4 days, to remove the LP from the pores before SEM. Ice adhesion strength was tested in a vertical shear mode by Instron machine (model 5944) equipped with a home-built testing system, as described in our previous reports.[41,42] Before the testing, 5 mL of deionized water was first poured into a centrifuge tube, which was placed on the SLIPS. The centrifuge tube was sealed by a pressure of 200 g of metal cylinder to avoid water leakage. The specimens were then placed in a freezer at −18 °C for more than 2 h to form ice on the surface. Afterward, the specimens were transferred to the testing system and stabilized at −18 °C for 30 min before loading. The force probe was closed to the surface (<1 mm) and loaded with a speed of 0.01 mm s^{-1}. During icing/deicing cycles, the samples were placed at room temperature for 30 min to recover before the next icing process.

ASSOCIATED CONTENT

Supporting Information

The Supporting Information is available free of charge on the ACS Publications website at DOI: 10.1021/acsomega.8b01148.

Regeneration process of LP-0.25 from 0 to 30 min and coalescence events of LP-0.25 (PDF)

Regeneration process of droplets from 0 to 30 min (AVI)

Coalescence events contributing to the growth of droplets (AVI)

AUTHOR INFORMATION

Corresponding Authors

*E-mail: jianying.he@ntnu.no (J.H.).
*E-mail: zhiliang.zhang@ntnu.no (Z.Z.).

ORCID

Yizhi Zhuo: 0000-0003-1415-3561
Jianying He: 0000-0001-8485-7893
Zhiliang Zhang: 0000-0002-9557-3455

Notes

The authors declare no competing financial interest.

ACKNOWLEDGMENTS

The Research Council of Norway is acknowledged for the support to the PETROMAKS2 Project Durable Arctic Icephobic Materials (project no. 255507), the FRINATEK Project Towards Design of Super-Low Ice Adhesion Surfaces(project no. 250990), and for the support to the Norwegian Micro- and Nano-Fabrication Facility, NorFab, project number 245963.

REFERENCES

(1) Mishchenko, L.; Hatton, B.; Bahadur, V.; Taylor, J. A.; Krupenkin, T.; Aizenberg, J. Design of Ice-Free Nanostructured Surfaces Based on Repulsion of Impacting Water Droplets. *ACS Nano* **2010**, *4*, 7699−7707.

(2) Kreder, M. J.; Alvarenga, J.; Kim, P.; Aizenberg, J. Design of Anti-icing Surfaces: Smooth, Textured or Slippery? *Nat. Rev. Mater.* **2016**, *1*, 15003.

(3) Liu, B.; Zhang, K.; Tao, C.; Zhao, Y.; Li, X.; Zhu, K.; Yuan, X. Strategies for Anti-Icing: Low Surface Energy or Liquid-Infused? *RSC Adv.* **2016**, *6*, 70251−70260.

(4) Sojoudi, H.; Wang, M.; Boscher, N. D.; McKinley, G. H.; Gleason, K. K. Durable and Scalable Icephobic Surfaces: Similarities and Distinctions from Superhydrophobic surfaces. *Soft Matter* **2016**, *12*, 1938−1963.

(5) Maitra, T.; Tiwari, M. K.; Antonini, C.; Schoch, P.; Jung, S.; Eberle, P.; Poulikakos, D. On the Nanoengineering of Superhydrophobic and Impalement Resistant Surface Textures Below the Freezing Temperature. *Nano Lett.* **2014**, *14*, 172−182.

(6) Wen, M.; Wang, L.; Zhang, M.; Jiang, L.; Zheng, Y. Antifogging and Icing-Delay Properties of Composite Micro- and Nanostructured Surfaces. *ACS Appl. Mater. Interfaces* **2014**, *6*, 3963−3968.

(7) Boinovich, L.; Emelyanenko, A. M.; Korolev, V. V.; Pashinin, A. S. Effect of Wettability on Sessile Drop Freezing: When Superhydrophobicity Stimulates an Extreme Freezing Delay. *Langmuir* **2014**, *30*, 1659−1668.

(8) Maitra, T.; Jung, S.; Giger, M. E.; Kandrical, V.; Ruesch, T.; Poulikakos, D. Superhydrophobicity vs. Ice Adhesion: The Quandary of Robust Icephobic Surface Design. *Adv. Mater. Interfaces* **2015**, *2*, 1500330.

(9) Dotan, A.; Dodiuk, H.; Laforte, C.; Kenig, S. The Relationship Between Water Wetting and Ice Adhesion. *J. Adhes. Sci. Technol.* **2009**, *23*, 1907−1915.

(10) Tang, Y.; Zhang, Q.; Zhan, X.; Chen, F. Superhydrophobic and Anti-Icing Properties at Overcooled Temperature of a Fluorinated Hybrid Surface Prepared via a Sol-Gel Process. *Soft Matter* **2015**, *11*, 4540−4550.

(11) Zhan, X.; Yan, Y.; Zhang, Q.; Chen, F. A Novel Superhydrophobic Hybrid Nanocomposite Material Prepared by Surface-Initiated AGET ATRP and its Anti-Icing Properties. *J. Mater. Chem. A* **2014**, *2*, 9390−9399.

DOI: 10.1021/acsomega.8b01148
ACS Omega 2018, 3, 10139−10144

(12) Wang, L.; Gong, Q.; Zhan, S.; Jiang, L.; Zheng, Y. Robust Anti-Icing Performance of a Flexible Superhydrophobic Surface. *Adv. Mater.* **2016**, *28*, 7729−7735.
(13) Zhu, L.; Shi, P.; Xue, J.; Wang, Y.; Chen, Q.; Ding, J.; Wang, Q. Superhydrophobic Stability of Nanotube Array Surfaces under Impact and Static Forces. *ACS Appl. Mater. Interfaces* **2014**, *6*, 8073−8079.
(14) Bharathidasan, T.; Kumar, S. V.; Bobji, M. S.; Chakradhar, R. P. S.; Basu, B. J. Effect of Wettability and Surface Roughness on Ice-Adhesion Strength of Hydrophilic, Hydrophobic and Superhydrophobic Surfaces. *Appl. Surf. Sci.* **2014**, *314*, 241−250.
(15) Golovin, K.; Kobaku, S. P. R.; Lee, D. H.; DiLoreto, E. T.; Mabry, J. M.; Tuteja, A. Designing Durable Icephobic Surfaces. *Sci. Adv.* **2016**, *2*, No. e1501496.
(16) Chen, J.; Liu, J.; He, M.; Li, K.; Cui, D.; Zhang, Q.; Zeng, X.; Zhang, Y.; Wang, J.; Song, Y. Superhydrophobic Surfaces Cannot Reduce Ice adhesion. *Appl. Phys. Lett.* **2012**, *101*, 111603.
(17) Nosonovsky, M.; Hejazi, V. Why Superhydrophobic Surfaces Are Not Always Icephobic. *ACS Nano* **2012**, *6*, 8488−8491.
(18) Kim, P.; Wong, T.-S.; Alvarenga, J.; Kreder, M. J.; Adorno-Martinez, W. E.; Aizenberg, J. Liquid-infused Nanostructured Surfaces with Extreme Anti-Ice and Anti-Frost Performance. *ACS Nano* **2012**, *6*, 6569−6577.
(19) Wong, T.-S.; Kang, S. H.; Tang, S. K. Y.; Smythe, E. J.; Hatton, B. D.; Grinthal, A.; Aizenberg, J. Bioinspired Self-Repairing Slippery Surfaces with Pressure-Stable Omniphobicity. *Nature* **2011**, *477*, 443−447.
(20) Subramanyam, S. B.; Rykaczewski, K.; Varanasi, K. K. Ice Adhesion on Lubricant-Impregnated Textured Surfaces. *Langmuir* **2013**, *29*, 13414−13418.
(21) Zhang, G.; Zhang, Q.; Cheng, T.; Zhan, X.; Chen, F. Polyols-Infused Slippery Surfaces Based on Magnetic Fe3O4-Functionalized Polymer Hybrids for Enhanced Multifunctional Anti-Icing and Deicing Properties. *Langmuir* **2018**, *34*, 4052−4058.
(22) Irajizad, P.; Hasnain, M.; Farokhnia, N.; Sajadi, S. M.; Ghasemi, H. Magnetic slippery extreme icephobic surfaces. *Nat. Commun.* **2016**, *7*, 13395.
(23) Coady, M. J.; Wood, M.; Wallace, G. Q.; Nielsen, K. E.; Kietzig, A.-M.; Lagugné-Labarthet, F.; Ragogna, P. J. Icephobic Behavior of UV-Cured Polymer Networks Incorporated into Slippery Lubricant-Infused Porous Surfaces: Improving SLIPS Durability. *ACS Appl. Mater. Interfaces* **2018**, *10*, 2890−2896.
(24) Jafari, R.; Momen, G.; Farzaneh, M. Durability Enhancement of Icephobic Fluoropolymer Film. *J. Coat. Technol. Res.* **2016**, *13*, 405−412.
(25) Ghalmi, Z.; Farzaneh, M. Durability of Nanostructured Coatings Based on PTFE Nanoparticles Deposited on Porous Aluminum Alloy. *Appl. Surf. Sci.* **2014**, *314*, 564−569.
(26) Liu, Q.; Yang, Y.; Huang, M.; Zhou, Y.; Liu, Y.; Liang, X. Durability of a Lubricant-Infused Electrospray Silicon Rubber Surface as an Anti-Icing Coating. *Appl. Surf. Sci.* **2015**, *346*, 68−76.
(27) Chen, J.; Dou, R.; Cui, D.; Zhang, Q.; Zhang, Y.; Xu, F.; Zhou, X.; Wang, J.; Song, Y.; Jiang, L. Robust Prototypical Anti-Icing Coatings with a Self-Lubricating Liquid Water Layer between Ice and Substrate. *ACS Appl. Mater. Interfaces* **2013**, *5*, 4026−4030.
(28) Chen, J.; Luo, Z.; Fan, Q.; Lv, J.; Wang, J. Anti-ice Coating Inspired by Ice Skating. *Small* **2014**, *10*, 4693−4699.
(29) Sun, X.; Damle, V. G.; Liu, S.; Rykaczewski, K. Bioinspired Stimuli-Responsive and Antifreeze-Secreting Anti-Icing Coatings. *Adv. Mater. Interfaces* **2015**, *2*, 1400479.
(30) Liu, W.; Chen, Z.; Zhou, G.; Sun, Y.; Lee, H. R.; Liu, C.; Yao, H.; Bao, Z.; Cui, Y. 3D Porous Sponge-Inspired Electrode for Stretchable Lithium-Ion Batteries. *Adv. Mater.* **2016**, *28*, 3578−3583.
(31) Kang, S.; Lee, J.; Lee, S.; Kim, S.; Kim, J.-K.; Algadi, H.; Al-Sayari, S.; Kim, D.-E.; Kim, D.; Lee, T. Highly Sensitive Pressure Sensor Based on Bioinspired Porous Structure for Real-Time Tactile Sensing. *Adv. Electron. Mater.* **2016**, *2*, 1600356.
(32) Zhao, X.; Li, L.; Li, B.; Zhang, J.; Wang, A. Durable Superhydrophobic/Superoleophilic PDMS Sponges and their Applications in Selective Oil Absorption and in Plugging Oil Leakages. *J. Mater. Chem. A* **2014**, *2*, 18281−18287.
(33) Giustiniani, A.; Guégan, P.; Marchand, M.; Poulard, C.; Drenckhan, W. Generation of Silicone Poly-HIPEs with Controlled Pore Sizes via Reactive Emulsion Stabilization. *Macromol. Rapid Commun.* **2016**, *37*, 1527−1532.
(34) Tebboth, M.; Jiang, Q.; Kogelbauer, A.; Bismarck, A. Inflatable Elastomeric Macroporous Polymers Synthesized from Medium Internal Phase Emulsion Templates. *ACS Appl. Mater. Interfaces* **2015**, *7*, 19243−19250.
(35) Zhao, J.; Luo, G.; Wu, J.; Xia, H. Preparation of Microporous Silicone Rubber Membrane with Tunable Pore Size via Solvent Evaporation-Induced Phase Separation. *ACS Appl. Mater. Interfaces* **2013**, *5*, 2040−2046.
(36) Jung, S.; Kim, J. H.; Kim, J.; Choi, S.; Lee, J.; Park, I.; Hyeon, T.; Kim, D.-H. Reverse-Micelle-Induced Porous Pressure-Sensitive Rubber for Wearable Human-Machine Interfaces. *Adv. Mater.* **2014**, *26*, 4825−4830.
(37) Duan, S.; Yang, K.; Wang, Z.; Chen, M.; Zhang, L.; Zhang, H.; Li, C. Fabrication of Highly Stretchable Conductors Based on 3D Printed Porous Poly(dimethylsiloxane) and Conductive Carbon Nanotubes/Graphene Network. *ACS Appl. Mater. Interfaces* **2016**, *8*, 2187−2192.
(38) Zhu, D.; Handschuh-Wang, S.; Zhou, X. Recent Progress in Fabrication and Application of Polydimethylsiloxane Sponges. *J. Mater. Chem. A* **2017**, *5*, 16467−16497.
(39) Wang, Y.; Yao, X.; Wu, S.; Li, Q.; Lv, J.; Wang, J.; Jiang, L. Bioinspired Solid Organogel Materials with a Regenerable Sacrificial Alkane Surface Layer. *Adv. Mater.* **2017**, *29*, 1700865.
(40) Zhuo, Y.; Håkonsen, V.; He, Z.; Xiao, S.; He, J.; Zhang, Z. Enhancing the Mechanical Durability of Icephobic Surfaces by Introducing Autonomous Self-Healing Function. *ACS Appl. Mater. Interfaces* **2018**, *10*, 11972−11978.
(41) He, Z.; Xiao, S.; Gao, H.; He, J.; Zhang, Z. Multiscale Crack Initiator Promoted Super-Low Ice Adhesion Surfaces. *Soft Matter* **2017**, *13*, 6562−6568.
(42) He, Z.; Vågenes, E. T.; Delabahan, C.; He, J.; Zhang, Z. Room Temperature Characteristics of Polymer-Based Low Ice Adhesion Surfaces. *Sci. Rep.* **2017**, *7*, 42181.
(43) He, Z.; Zhuo, Y.; He, J.; Zhang, Z. Design and Preparation of Sandwich-Like Polydimethylsiloxane (PDMS) Sponges with Super-Low Ice Adhesion. *Soft Matter* **2018**, *14*, 4846.
(44) Hejazi, V.; Sobolev, K.; Nosonovsky, M. From Superhydrophobicity to Icephobicity: Forces and Interaction Analysis. *Sci. Rep.* **2013**, *3*, 2194.
(45) Chen, D.; Gelenter, M. D.; Hong, M.; Cohen, R. E.; McKinley, G. H. Icephobic Surfaces Induced by Interfacial Nonfrozen Water. *ACS Appl. Mater. Interfaces* **2017**, *9*, 4202−4214.
(46) Wang, Y.; Yao, X.; Chen, J.; He, Z.; Liu, J.; Li, Q.; Wang, J.; Jiang, L. Organogel as Durable Anti-icing Coatings. *Sci. China Mater.* **2015**, *58*, 559−565.

DOI: 10.1021/acsomega.8b01148
ACS Omega 2018, 3, 10139−10144